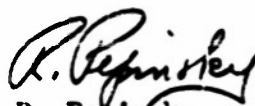


AD No. 10374
ASTIA FILE COPY

Study of Phase Transitions
in Perovskite-Type Crystals

Gen Shirane and Ray Pepinsky

This report concerns developments supported at The Pennsylvania State College in part by Contract No. N6onr-26919 with the Acoustics Branch of the Office of Naval Research, and in part by Contract No. AF-33(038)-12645 with the Wright Air Development Center, Department of the Air Force. Crystal preparation and dielectric measurements were supported under both contracts; specific heat and X-ray measurements were supported by the Air Force Contract only.



R. Pepinsky
Projects Director
X-Ray and Solid State Laboratory
Department of Physics
The Pennsylvania State College
1 November 1952

Table of Contents

Abstract	1
A. Phase Transitions in PbHfO_3	2
I. Introduction	2
II. Specimen Preparation	3
III. Crystal Structure at Room Temperature	4
IV. Dielectric Properties	5
V. Structural Changes around the Phase Transitions	9
VI. Discussion	14
B. Study of NaNbO_3 - KNbO_3 System	17
I. Introduction	17
II. Dielectric Properties	18
III. Structural Study	24
IV. Specific Heat Measurements	26
V. Discussion	30
References	32

List of Illustrations

	Page No.
Fig. 1 Model of Atomic Arrangement in PbZrO_3 -----	6
Fig. 2 Powder Photographs of PbZrO_3 and PbHfO_3 -----	7
Fig. 3 Dielectric Constant of PbHfO_3 -----	8
Fig. 4 P vs. E Relations for PbHfO_3 -----	10
Fig. 5 Lattice Parameters of PbHfO_3 -----	12
Fig. 6 Axial ratio c/a of PbHfO_3 -----	13
Fig. 7 Phase Diagram of $\text{Pb}(\text{Zr-Ti})\text{O}_3$ -----	15
Fig. 8 Phase Diagram of $(\text{Pb-Ba})\text{ZrO}_3$ and $(\text{Pb-Sr})\text{ZrO}_3$ -----	16
Fig. 9 Dielectric constant of NaNbO_3 and $(\text{K}_{.05}\text{-Na}_{.95})\text{NbO}_3$ -----	19
Fig. 10 Dielectric constant of $(\text{K}_{.10}\text{-Na}_{.90})\text{NbO}_3$ and $(\text{K}_{.50}\text{-Na}_{.50})\text{NbO}_3$ -	20
Fig. 11 Dielectric constant of KNbO_3 -----	21
Fig. 12 Phase diagram of $(\text{K-Na})\text{NbO}_3$ -----	22
Fig. 13 P vs. E Relations for $(\text{K-Na})\text{NbO}_3$ -----	23
Fig. 14 Specific Heat of KNbO_3 -----	27
Fig. 15 Specific Heat of $(\text{K}_{.10}\text{-Na}_{.90})\text{NbO}_3$ -----	28
Fig. 16 Specific Heat of NaNbO_3 -----	29

STUDY OF PHASE TRANSITIONS IN PEROVSKITE-TYPE CRYSTALS

The discovery of the ferroelectric activity of BaTiO_3 ⁽¹⁾ has attracted many researchers to further studies of related perovskite-type crystals with molecular formula ABO_3 . The perovskite-type crystals which have shown ferroelectric activity can be divided into at least three classes: one is $\text{A}^{+2}\text{B}^{+4}\text{O}_3$, such as BaTiO_3 ; the second is $\text{A}^{+1}\text{B}^{+5}\text{O}_3$, such as KNbO_3 ; and the third is $\text{A}^{+1}\text{A}^{+3}\text{B}_2^{+4}\text{O}_6$, such as $\text{KLa}(\text{TiO}_3)_2$. Other perovskite-type materials have also been examined elsewhere, but their characteristics are not considered here because we have had no experience with them.

In the first group we have been studying the properties of PbHfO_3 , and have found that this crystal is an antiferroelectric of the same type as PbZrO_3 . In the second group we have been interested in the NaNbO_3 - KNbO_3 system, which shows very peculiar properties, and is discussed in some detail below.

A. PHASE TRANSITIONS IN PbHfO_3

I. INTRODUCTION.

Recent studies of PbTiO_3 ⁽²⁾ and PbZrO_3 ⁽³⁾ have revealed interesting dielectric properties and relations of these to the crystal structures of these perovskite-like compounds. PbTiO_3 is a ferroelectric with a Curie point of 490°C , and this is very similar to the much-studied Curie point of BaTiO_3 at 120°C . The crystal structure ⁽⁴⁾ of PbTiO_3 is distorted to a tetragonal lattice below its Curie point, and with $c/a=1.06$ at room temperature; it is of course cubic above its Curie point. The dielectric properties of PbZrO_3 , on the other hand, have shown that this crystal is not ferroelectric but rather antiferroelectric with a Curie point at 230°C , notwithstanding the close resemblance of the permittivity vs. temperature curve of this crystal to those of BaTiO_3 and PbTiO_3 . The crystal structure ⁽⁴⁾ of PbZrO_3 is distorted to a tetragonal cell, but the axial ratio c/a is less than unity (0.99) -- in contrast with BaTiO_3 and PbTiO_3 in which c/a is bigger than unity.

No satisfactory explanation has been given of the reason why such an essential difference in dielectric and structural properties can be observed in these very closely related perovskite crystals. Although there is no doubt that the large polarizability of the Pb ion in both compounds contributes to these peculiar phenomena, the essential difference in these compounds is the differences in ionic radii and polarizabilities of B ions in the ABO_3 crystals which have Pb as the common A ion. This fact suggests that the further study of lead compounds with different B ions, such as PbHfO_3 and PbThO_3 , may give more information about this interesting phenomenon. The Hf ion has a rather close ionic radius to Zr and, at the same time, a

different (probably larger) polarizability. Up to now, however, few studies were carried out on hafnium compounds because of difficulty of obtaining pure hafnium. We have carried out a dielectric and structural study of PbHfO_3 , and observe that this crystal shows antiferroelectric behavior of the same type as PbZrO_3 .

II. SPECIMEN PREPARATION.

Ceramic PbHfO_3 was prepared from PbCO_3 and HfO_2 . Equimolar proportions of these ingredients were mixed well and fired at about 1200°C after preliminary firing at about 1000°C . The specimen was pressed into a pellet with a pressure of about 10^8 gm/cm². The fired specimen is a hard ceramic with a yellowish color.

The first difficulty in obtaining good PbHfO_3 arises from the difficulty of obtaining pure HfO_2 . One gram of HfO_2 was supplied by Fairmount Chemical Co., which company claimed a purity of 99.5% HfO_2 , with 0.3% ZrO_2 and 0.2% TiO_2 . Rough estimation by spectrographic examination, carried out by Dr. R. Hayes of the Pennsylvania State College, indicating the existence of Zr in an amount from 0.03% to 0.3%. A second and rather unexpected difficulty is the very severe evaporation of PbO from the specimen during the course of firing. A similar difficulty was encountered in the case of PbTiO_3 , and also (more pronounced) in the case of PbZrO_3 . But in PbHfO_3 the evaporation is so severe that the color of the surface of the sintered specimen changes to white and the powder photograph of the surface material shows some weak diffraction lines due to HfO_2 . Though the small supply of HfO_2 did not allow us to develop a satisfactory method for preventing the evaporation, the following procedure was helpful in obtaining a rather good specimen. A

few percent of PbO was added in excess of equimolar proportion, and firing was carried out rather quickly in a Pt crucible with a cover to retard the evaporation of PbO. The white surface of ^{the} specimen was removed by polishing, and the uniform yellow interior part was used for the dielectric and structural studies. No chemical analysis was carried out of the final specimen, and this should ultimately be done.

III. CRYSTAL STRUCTURE AT ROOM TEMPERATURE.

Powder photographs of PbHfO_3 were taken with a Norelco powder camera (11.4 cm. diameter), using Cu $K\alpha$ radiation. Diffraction lines clearly show a distorted perovskite structure, and all multiplets can be well explained by assuming a tetragonal cell with $c/a < 1$. The lattice constant and axial ratio calculated from (510), (431) and (422) lines are shown below, together with data for PbTiO_3 and PbZrO_3 .

Table I

Crystal	a-axis	c/a	unit cell volume
PbTiO_3	3.905	1.063	63.30
PbZrO_3	4.159	0.988	71.06
PbHfO_3	4.136	0.991	70.06

($\lambda = 1.5405 \text{ \AA}$ was used as the Cu $K\alpha_1$ wave length. The values for PbZrO_3 and PbTiO_3 were recalculated from Megaw's⁽⁴⁾ data with this wave length.)

It is to be noted here that the c/a ratio for PbHfO_3 is less than unity, as in PbZrO_3 . Moreover, some extra lines can be observed in the PbHfO_3 powder photograph besides the main lines due to a perovskite structure. Careful

**BEST
AVAILABLE
COPY**

comparison of these extra lines with those of PbZrO_3 showed essentially the same character of superstructure line not only in spacing but also in relative intensities. These facts strongly suggest that PbHfO_3 has the same type of superstructure as PbZrO_3 , which latter was studied by Sawaguchi et al.⁽⁵⁾ using a single crystal method. These investigators found an antiparallel displacement of Zr (or Pb) ions as shown in Fig. 1. Thus we can expect antiferroelectricity in PbHfO_3 similar to that in PbZrO_3 . Rough estimation of the intensities of diffraction patterns of these two crystals are shown in Fig. 2. Superstructure lines are indicated by open circles.

Besides these very close resemblances between the x-ray powder patterns of these two compounds, we can find a large difference in the ratio of the intensity of odd $N = h^2 + K^2 + L^2$ to that of even N , as easily seen in Fig. 2. This can be explained well by the difference in the atomic scattering factors of Zr and Hf. Another interesting result is that the unit cell volume of PbHfO_3 is smaller than PbZrO_3 , which obviously shows that the Hf 4^+ ion is slightly smaller than Zr 4^+ ion.

IV. DIELECTRIC PROPERTIES.

The specimen for dielectric measurement was a disk 1 mm. in thickness and 2.3 cm.² in area, and silver paste was applied to both surfaces as electrodes. Fig. 3 shows the dielectric constant vs. temperature curve at a frequency of 10 kc/sec.

This curve shows two anomalies in the temperature dependence of dielectric constant: one is a small anomaly at 160°C, which suggests the existence of some kind of phase change; another is a pronounced peak at 210°C, above which the crystal becomes paraelectric. From the crystal structure we

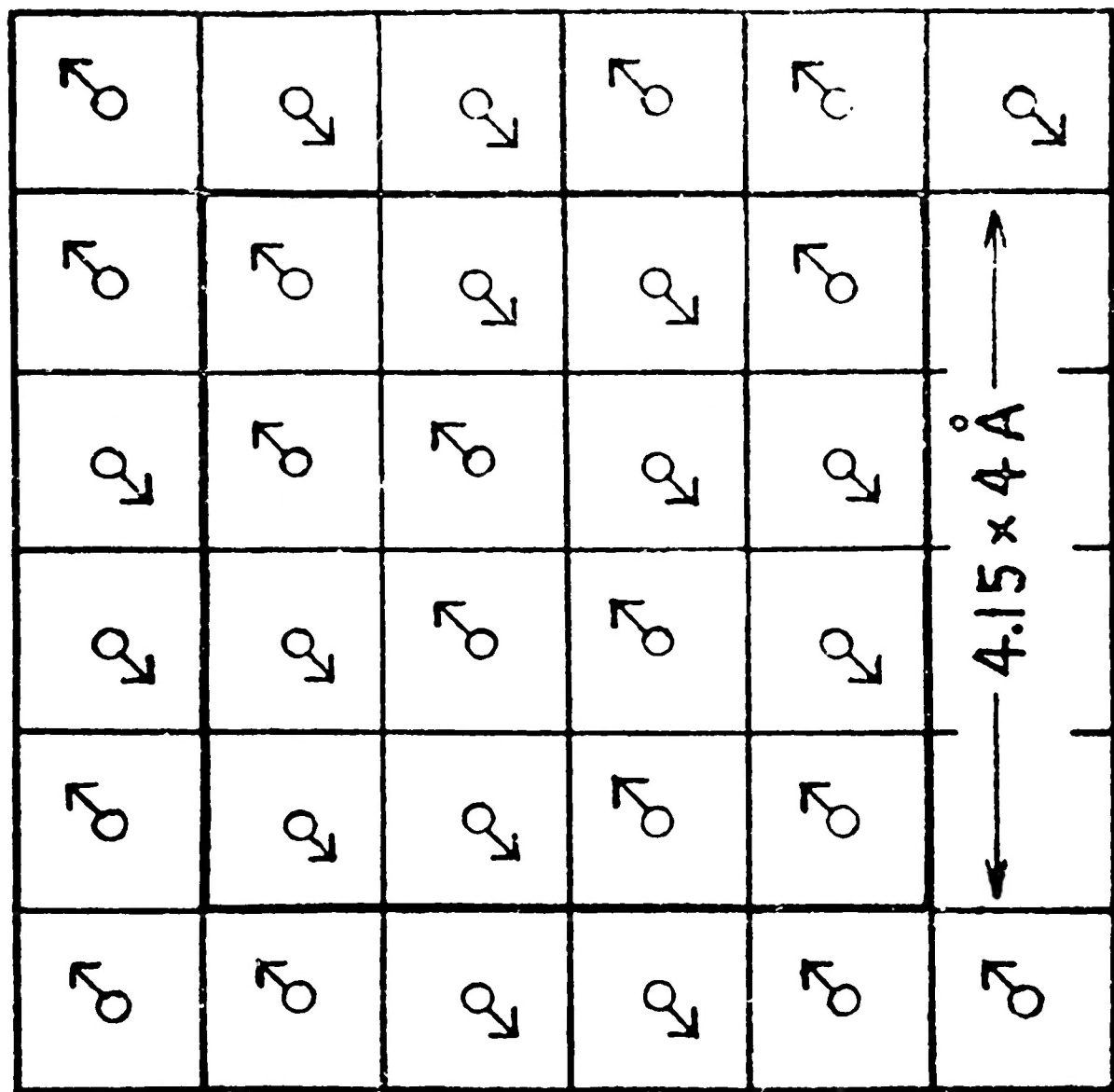


FIG. 1 A model of the atomic arrangement of PbZrO_3 , (001) plane. Although the true symmetry may be orthorhombic, we choose here tetragonal axes. An arrow shows the displacement of a heavy ion (probably a Pb ion).

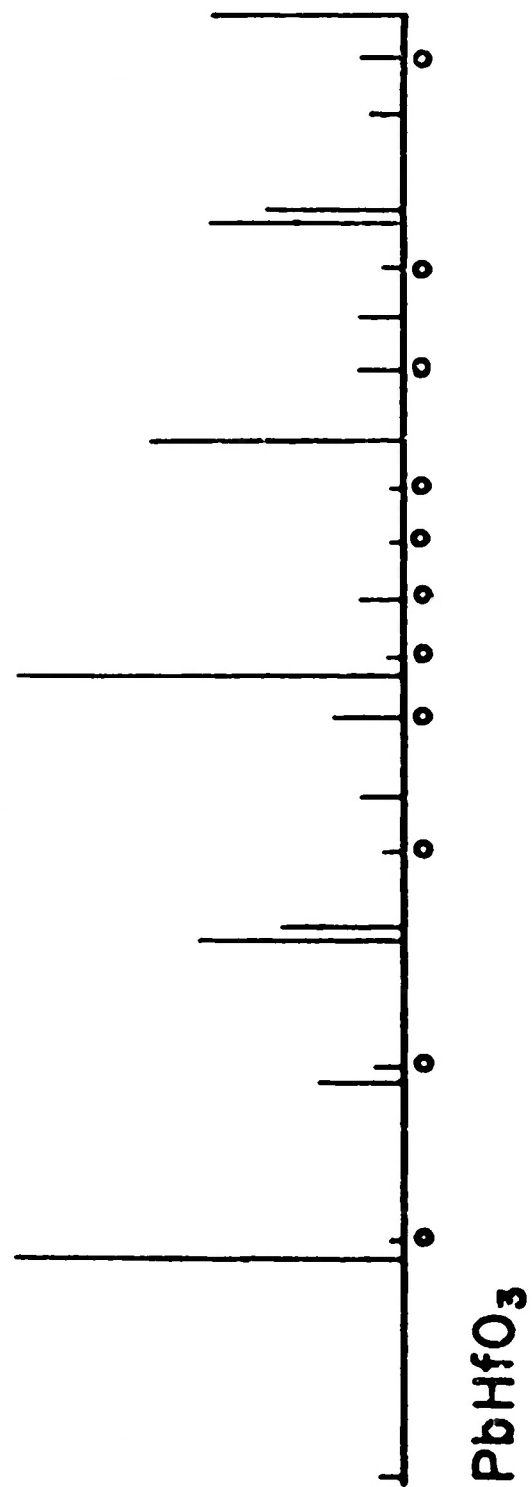
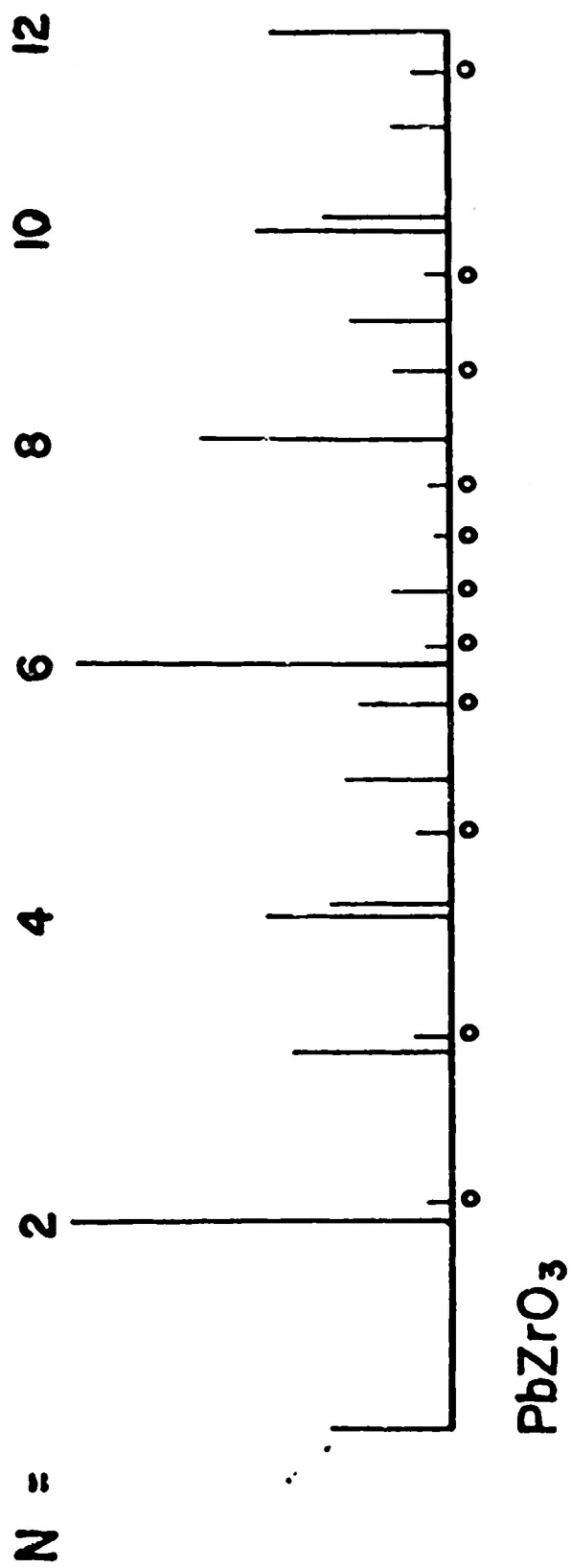


Fig. 2

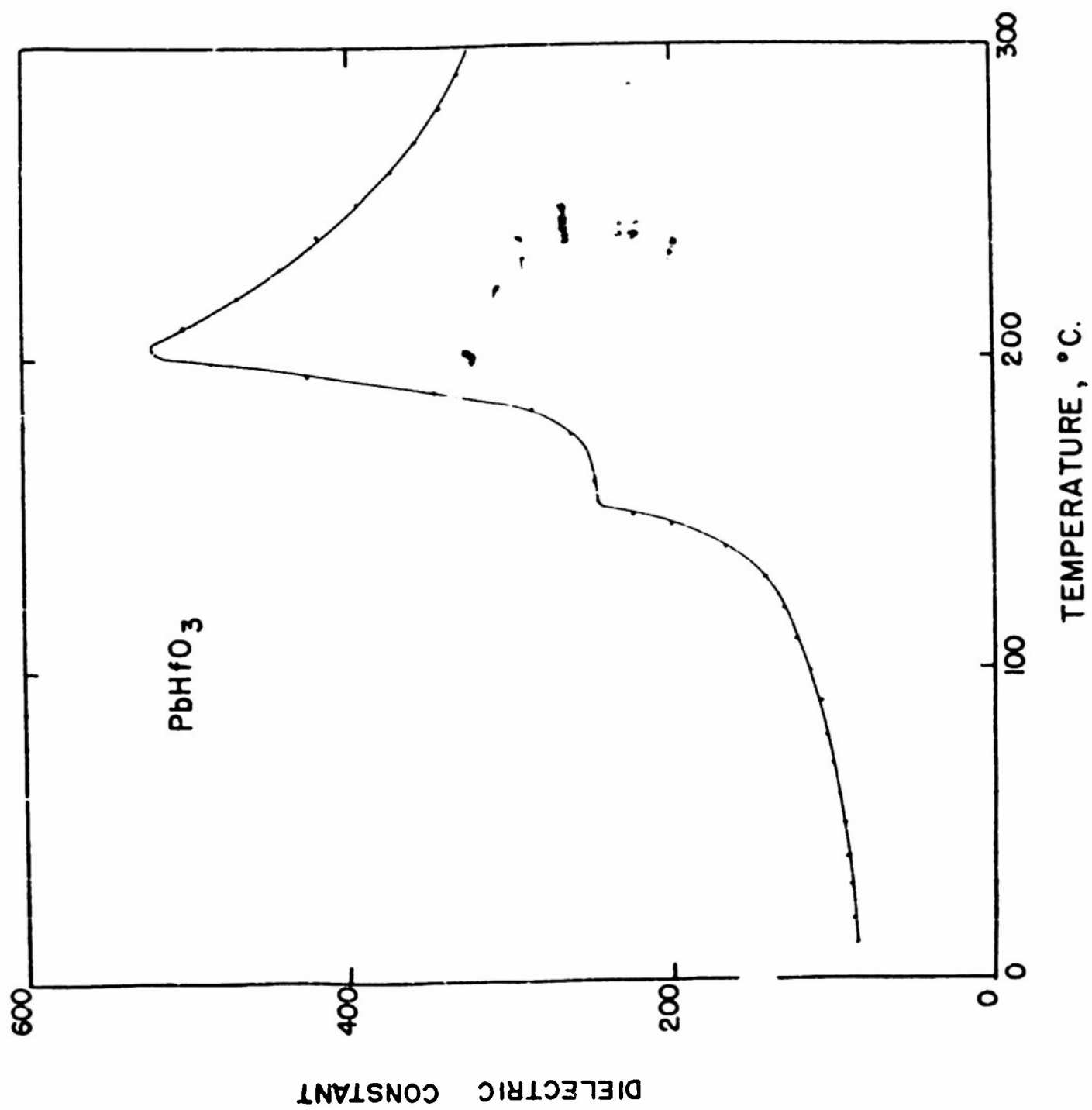


Fig. 3

can expect antiferroelectric properties in the phase below 160°C , and there is no doubt above the paraelectricity above 210°C . To study the dielectric response of the intermediate phase we examined the polarization vs. electric field relation under an a.c. amplitude of 10 kV/cm. As shown in Fig. 1, the P-E relation is almost linear in all three phases except for a slight upward curvature just below the Curie point. No ferroelectric hysteresis loops were observed even just below the Curie point.

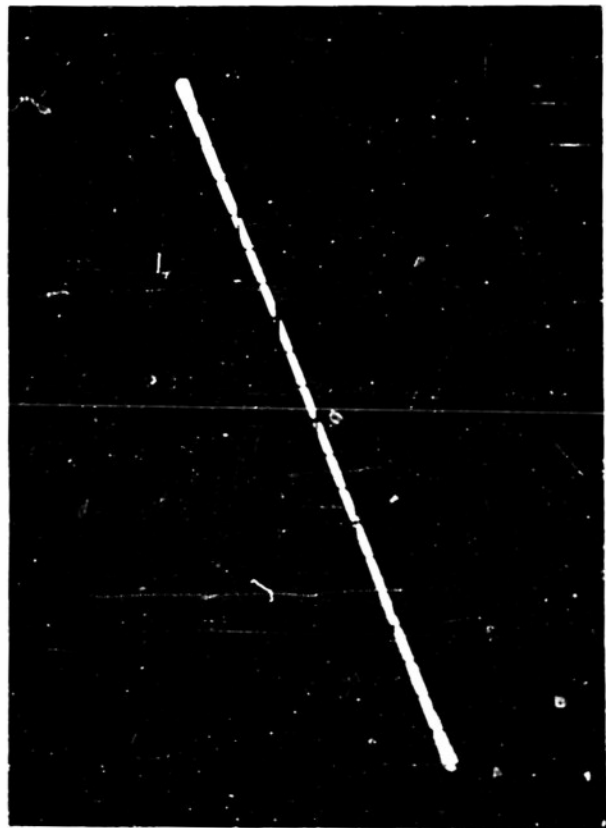
From this we can conclude that the lowest phase below 160°C is an antiferroelectric phase as observed in PbZrO_3 (phase AI) and that the intermediate phase is another antiferroelectric phase (AII) which must differ from phase AI in some way.

Above the Curie point the temperature dependence of the dielectric constant obeys the Curie-Weiss law $\epsilon = 1/(\chi - T_0)$, with $\chi = 1.0 \times 10^5$, $T_0 = 110^{\circ}\text{C}$; this Curie constant is very close to those of BaTiO_3 and PbZrO_3 .

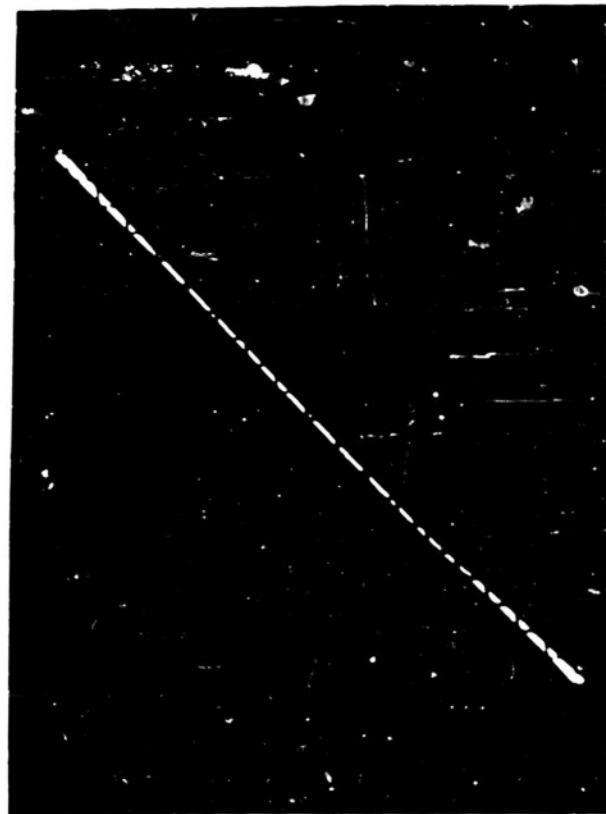
V. STRUCTURAL CHANGES AROUND THE PHASE TRANSITION

As shown in Fig. 3, the dielectric constant vs. temperature curve shows two anomalies, indicating two phase changes. Now, the interesting problem is the crystal structure of PbHfO_3 in the intermediate phase between these two phase changes at 160°C and 210°C . To check this point, a series of powder photographs at various temperatures were taken by using the Unicam (19 cm.) high-temperature X-ray powder camera.

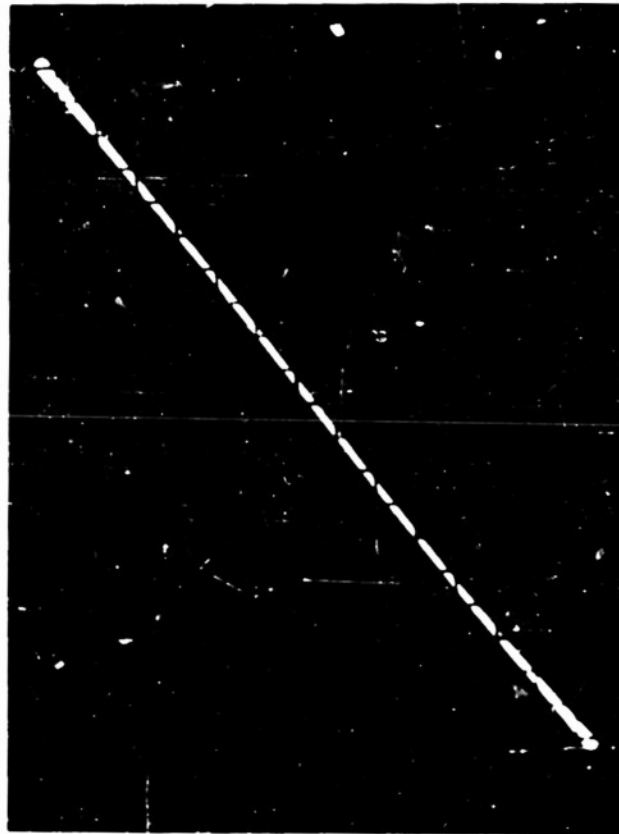
Below 160°C the diffraction patterns are essentially the same as at room temperature, except that the c/a ratio tends toward unity and, at the same time, the intensity of extra lines decrease gradually as 160°C is



30 °C.



170 °C.



200 °C.



220 °C.

Fig. 4.

P-E RELATION OF PbHfO_3

approached from below. Above 210°C the photographs show a cubic perovskite lattice without any superstructure lines.

The diffraction patterns at the temperature region in the intermediate phase is very close to a cubic pattern, and we can observe multiplets only in a few high-angle lines. In such a case it is rather difficult to determine the structure by using powder photographs only, and we tried to explain these multiplets only in a few high-angle lines, by assuming simple possible cases such as tetragonal $c/a > 1$, orthorhombic and rhombohedral. We found that the multiplets can be well explained if we assume a tetragonal lattice with $c/a < 1$. The lattice parameters and c/a calculated from (510), (431) and (422) lines are shown in Fig. 5 and Fig. 6.

The dielectric test showed that the dielectric properties of this middle phase may be antiferroelectric. Careful examination of powder photographs reveals a few rather weak but definite superstructure lines, which are different from those found at room temperature both in spacing and in relative intensity.

The above results show that the change at 160°C is a phase transformation from tetragonal to another tetragonal phase, with a discontinuity in the axial ratio c/a . This seems rather strange. However, we must notice here that the powder pattern at room temperature indicates a tetragonal lattice with $c/a < 1$; but the structural study of a single crystal of PbZrO_3 showed, as seen in Fig. 1, that the true symmetry of the crystal is not tetragonal but orthorhombic. We can conclude that the phase transition at 160°C is a phase change from orthorhombic phase to a tetragonal phase, caused by some rearrange-

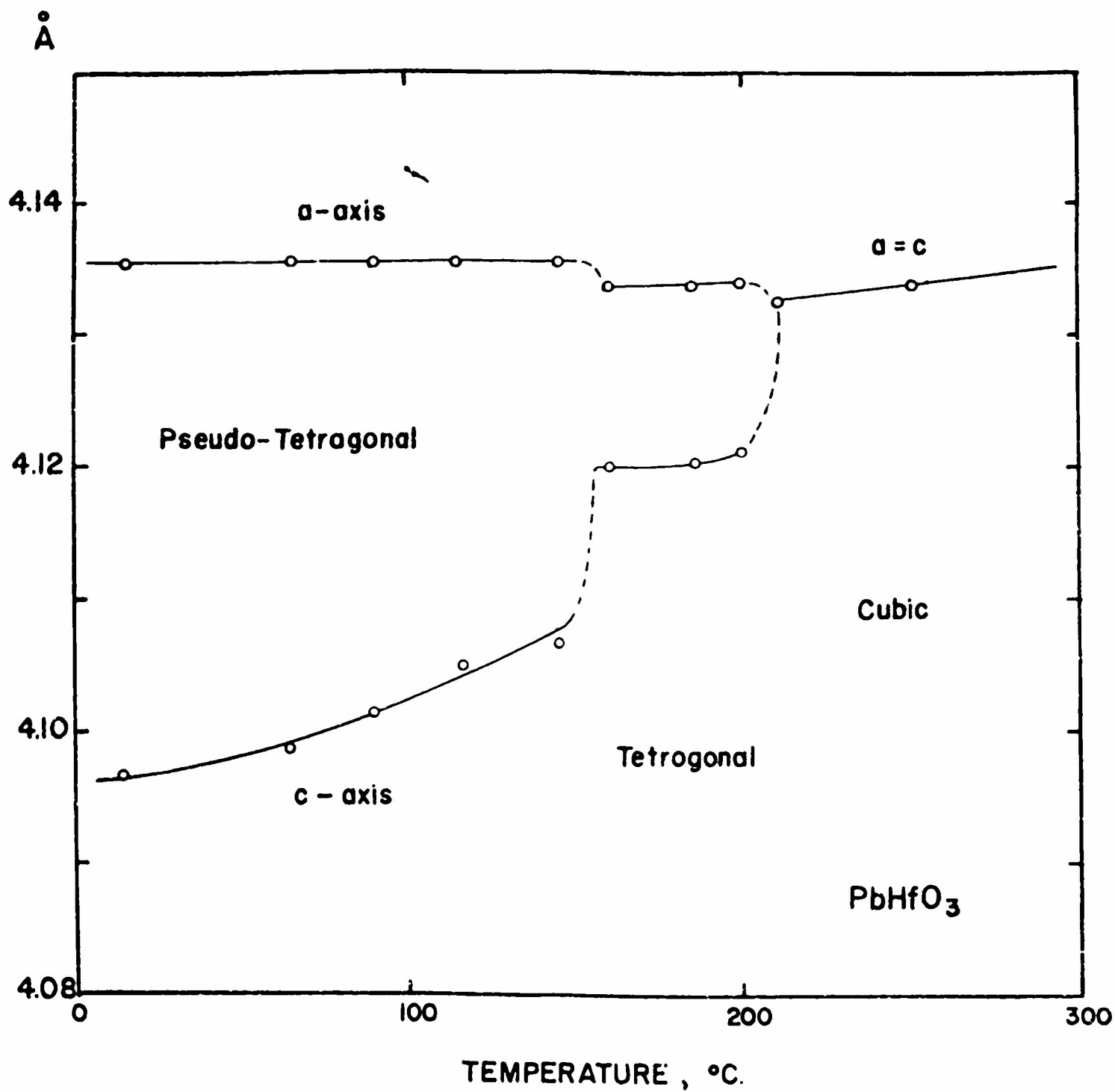


Fig. 5

LATTICE PARAMETERS OF PbHfO_3

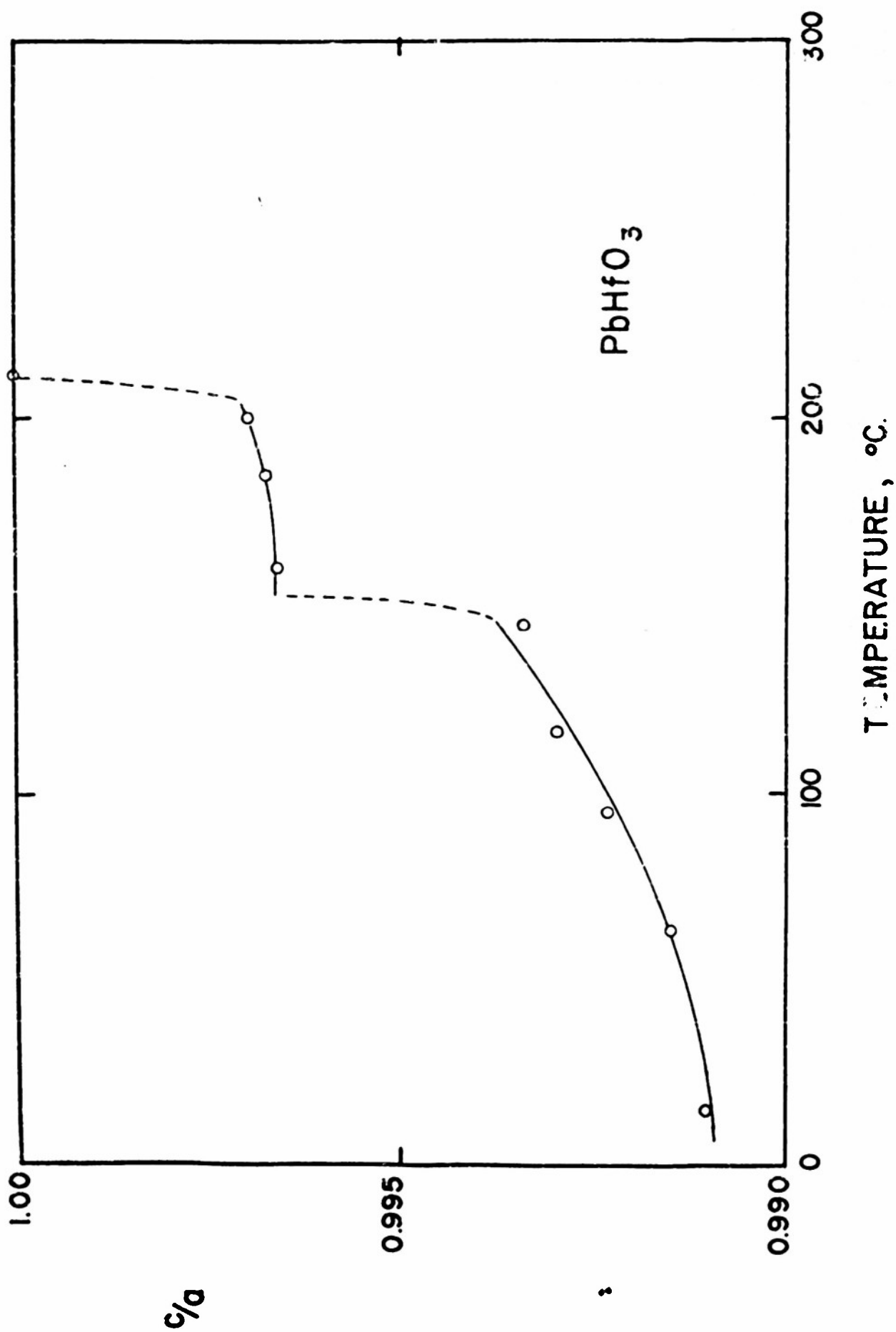
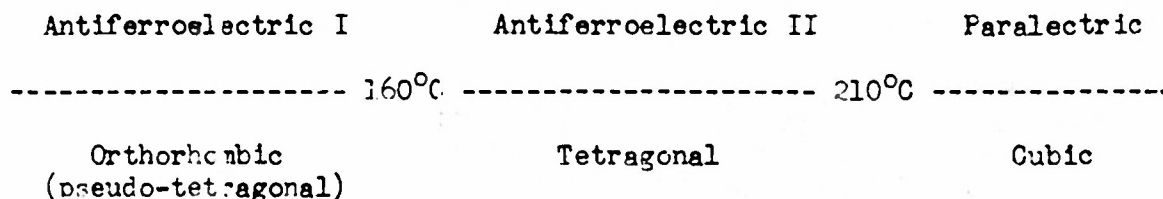


Fig. 6
AXIAL RATIO c/a OF PbHfO_3

ment of the antiparallel displacement of ions. The detailed study of the crystal structure of the intermediate phase must await single crystal study.

Summarizing, the phase changes in PbHfO_3 are shown in schematical form as follows:



VI. DISCUSSION.

The foregoing experimental results has shown that PbHfO_3 is antiferroelectric with a Curie point of 210°C. The interesting and rather unexpected results of these observations are: firstly, the Curie point of PbHfO_3 is very close to that of PbZrO_3 , notwithstanding the difference in the ionic radii and polarizabilities of these crystals; and, secondly, the existence of the antiferroelectric intermediate phase between the lowest and paraelectric phases. At present it is difficult to explain these facts; but the following consideration may be helpful.

The recent studies of PbZrO_3 ⁽³⁾ and solid solutions⁽⁶⁾ derived from PbZrO_3 by replacing Pb or Zr ions by other suitable ions show the rather peculiar phase diagrams as shown in Figs. 7 and 8. In the cases of $\text{Pb}(\text{Zr-Ti})\text{O}_3$ and $(\text{Pb-Ba})\text{ZrO}_3$, the rhombohedral ferroelectric intermediate phase was observed, and, on the other hand, in the case of $(\text{Pb-Sr})\text{ZrO}_3$, the tetragonal antiferroelectric intermediate phase was found. A comparison of superstructure lines in the intermediate phases of $(\text{Pb-Sr})\text{ZrO}_3$ and PbHfO_3 showed that the both compounds have essentially the same superstructure; consequently they are probably the same phase.

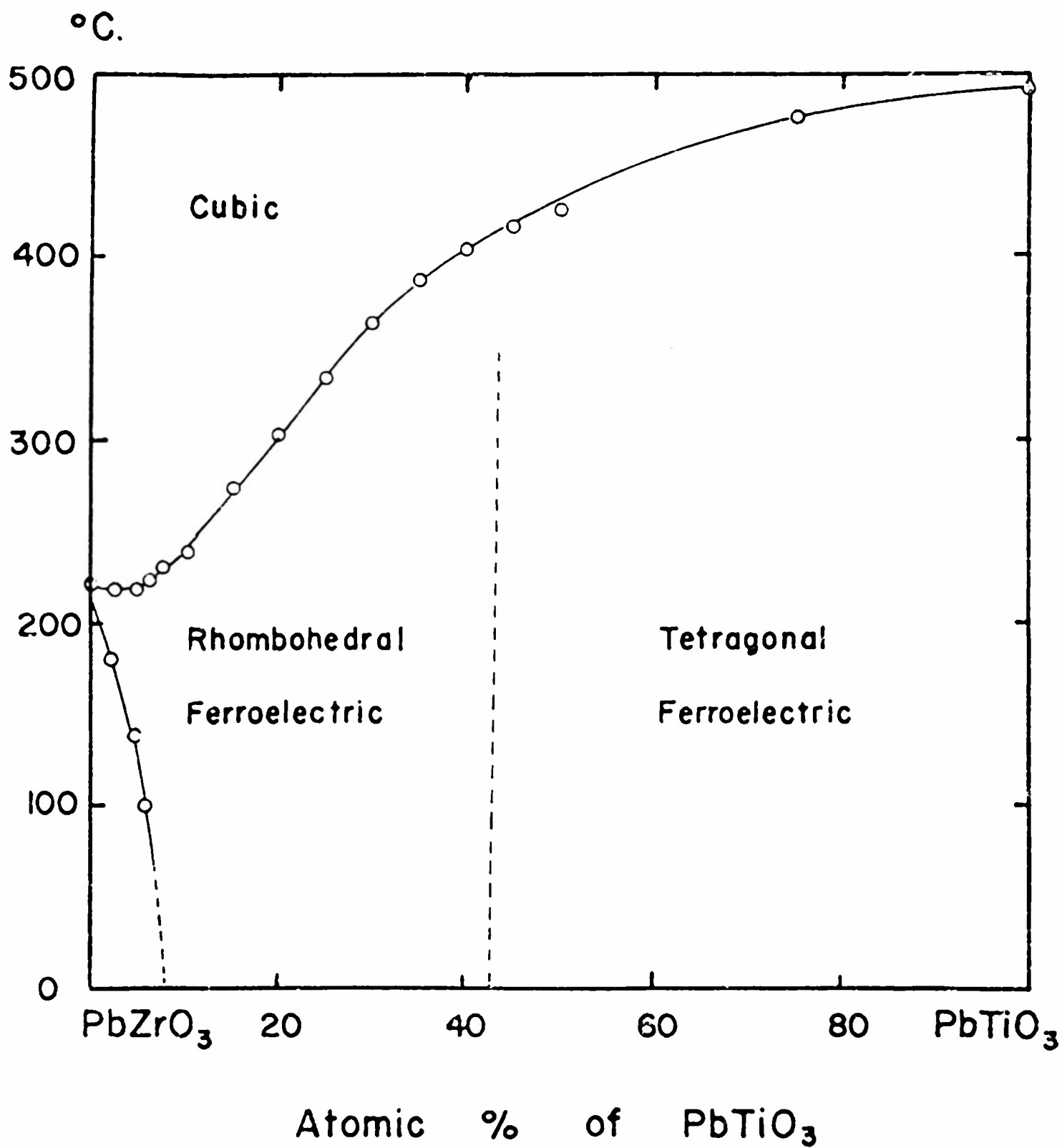


Fig. 7

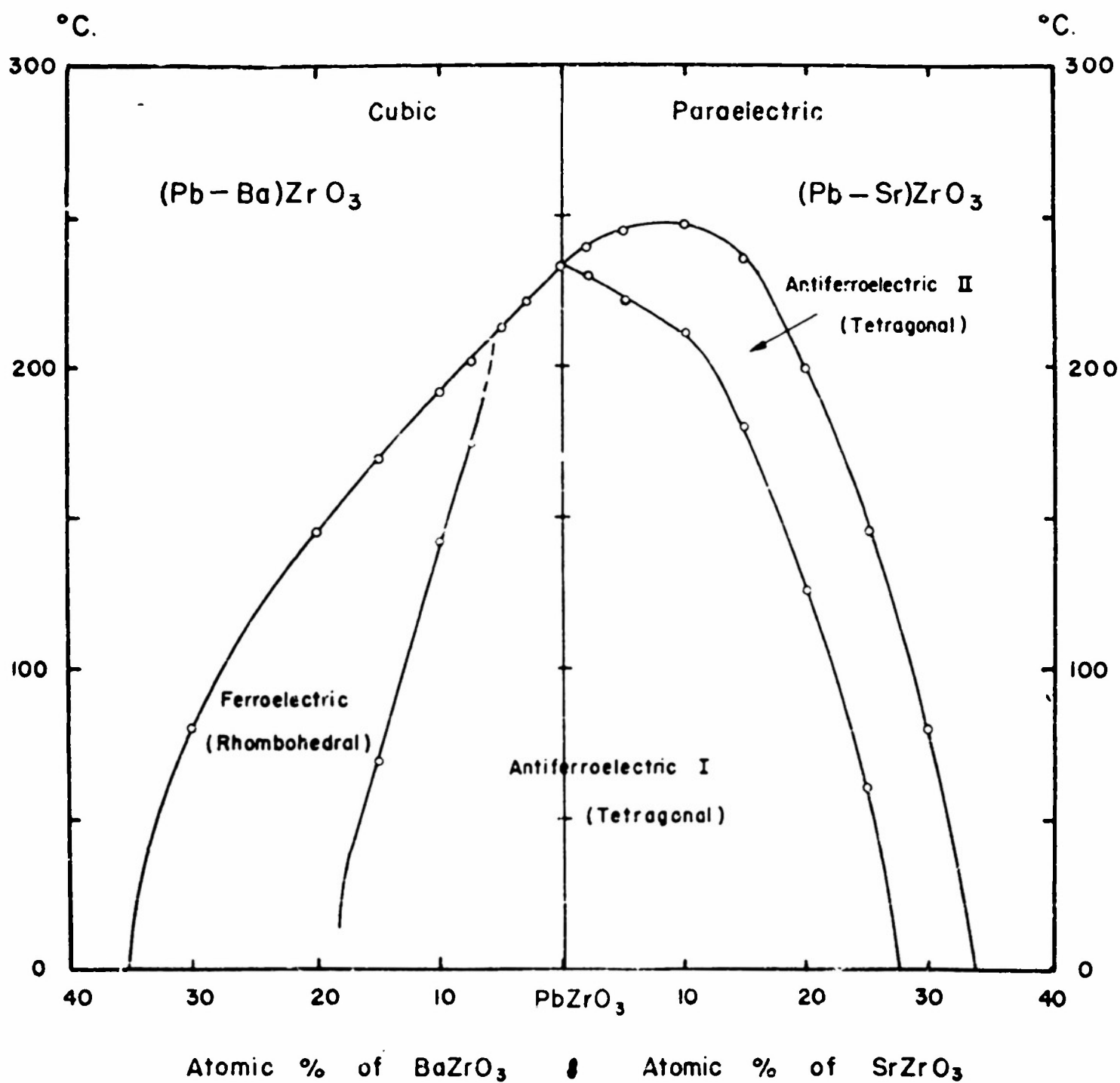


Fig. 8

Proper explanations of these many experimental results are not yet possible. However, if we assume that the small ionic radius and large polarizability of Hf ion compared with those of PbZrO_3 have almost compensated each other, we can possibly explain -- or at least expect -- the small change of the Curie point from PbZrO_3 to PbHfO_3 , and the existence of the intermediate phase in PbHfO_3 .

B. STUDY OF NaNbO_3 - KNbO_3 SYSTEM

I. INTRODUCTION.

The ferroelectric phase transitions in perovskite niobates were studied by Matthias and Remeika⁽⁷⁾ and by Wood⁽⁸⁾, with the following results:

KNbO_3 : orthorhombic 220°C tetragonal 430°C cubic.

NaNbO_3 : orthorhombic 370°C tetragonal 480°C cubic.

Concerning KNbO_3 , a recent study⁽⁹⁾ in our laboratory has revealed the existence of a phase change at -20°C, showing the existence of a lower rhombohedral phase which gives this crystal the complete similarity to the phase changes in BaTiO_3 .

On the other hand, the situation with NaNbO_3 is rather confusing. First, structural study of this crystal at room temperature by Vousden⁽¹⁰⁾ showed the non-polar structure which rejects, in any case, the existence of ferroelectricity in this crystal. Second, the optical and X-ray studies by Wood has suggested another higher phase change around 640°C, in addition to two phase transitions at 370°C and 480°C; and an optical study by Vousden led that investigator to report two phase changes at 300°C and 600°C.

These two questions: whether NaNbO_3 is really ferroelectric or not, and what transitions really exist in NaNbO_3 at high temperatures, suggested

the need for a further study of NaNbO_3 and its solid solutions with KNbO_3 .

II. DIELECTRIC PROPERTIES.

The specimen used for the following experiments were prepared from K_2CO_3 , Na_2CO_3 and Nb_2O_5 . These ingredients were mixed in desired proportions and fired at various temperature, which varied from 1200°C for pure NaNbO_3 to 1000°C for pure KNbO_3 after preliminary calcination. It is rather difficult to obtain hard ceramics, especially toward the pure KNbO_3 side, but applying a large pressure to the pellet and adjusting the firing temperature to just below the melting point, we could obtain good ceramics which are hard enough for dielectric tests. Silver paste was applied to both surfaces as electrodes.

Dielectric constant vs. temperature curves were measured at 10 kc/sec and 10 v/cm. Some of the results are shown in Fig. 9 to 11. In NaNbO_3 we observed only one anomaly at 370°C , in contrast with the two phase changes at 370°C and 480°C previously reported by Matthias and Remeika. When we replace small amount of Na in NaNbO_3 by K, we observe two anomalies as shown in Fig. 9 for $(\text{K}_5\text{-Na}_{95})\text{NbO}_3$. With increasing K concentration, these two anomalies were observed always around 200°C and 400°C . The dielectric constant of pure KNbO_3 shows two anomalies at 320°C and 430°C , in good agreement with the previous data of Matthias and Remeika.

From these measurements, the phase diagram of $(\text{K-Na})\text{NbO}_3$ was obtained as shown in Fig. 12. To study the ferroelectricity of each phase shown in this diagram, we examined the hysteresis loops of a number of solid solutions, and some of the results are shown in Fig. 13. Above the highest phase line, as expected, the P-E relation is always linear. In the intermediate phase we can get good hysteresis loop even in the specimen near the pure NaNbO_3 side.

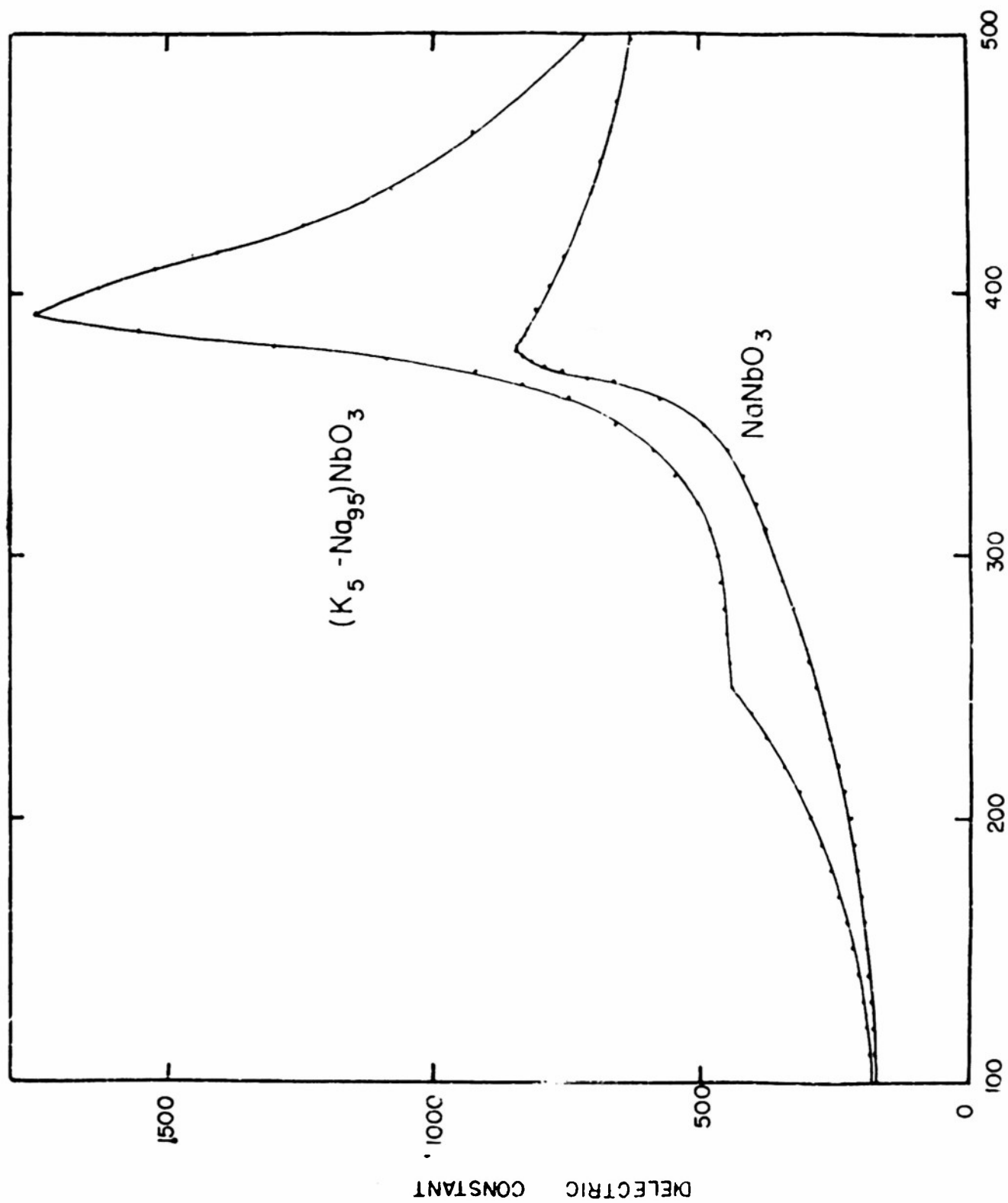


Fig. 9

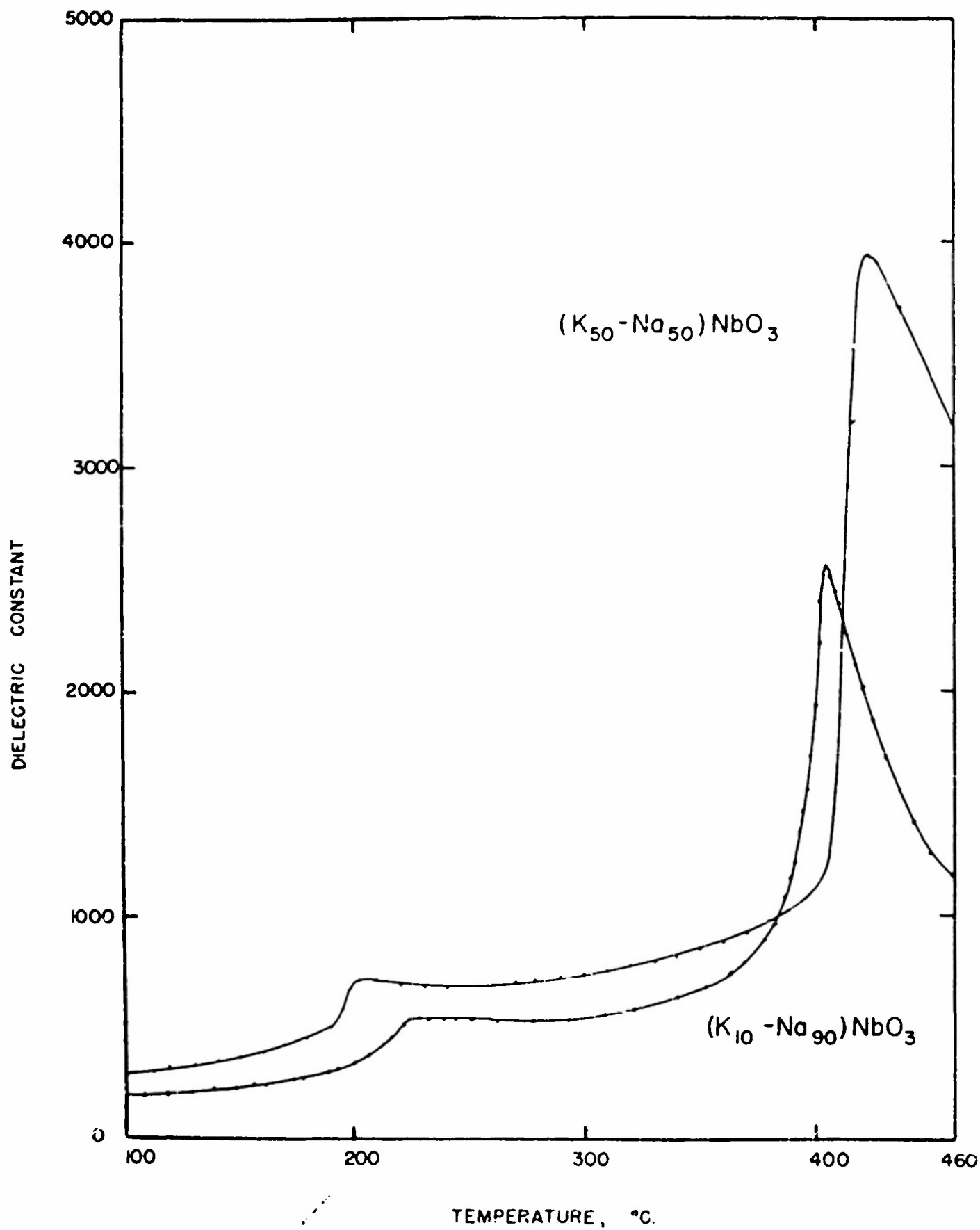


Fig. 10

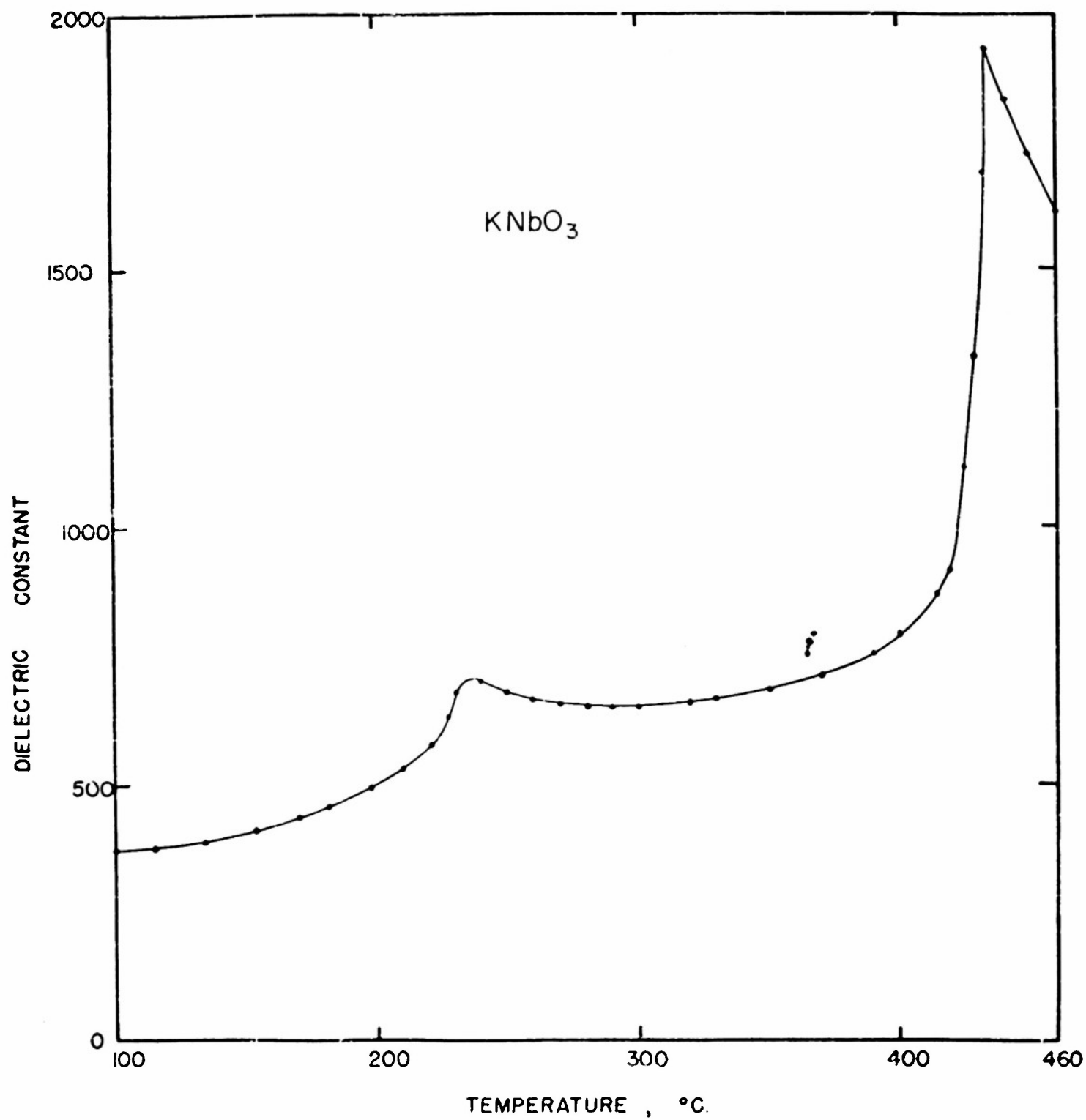
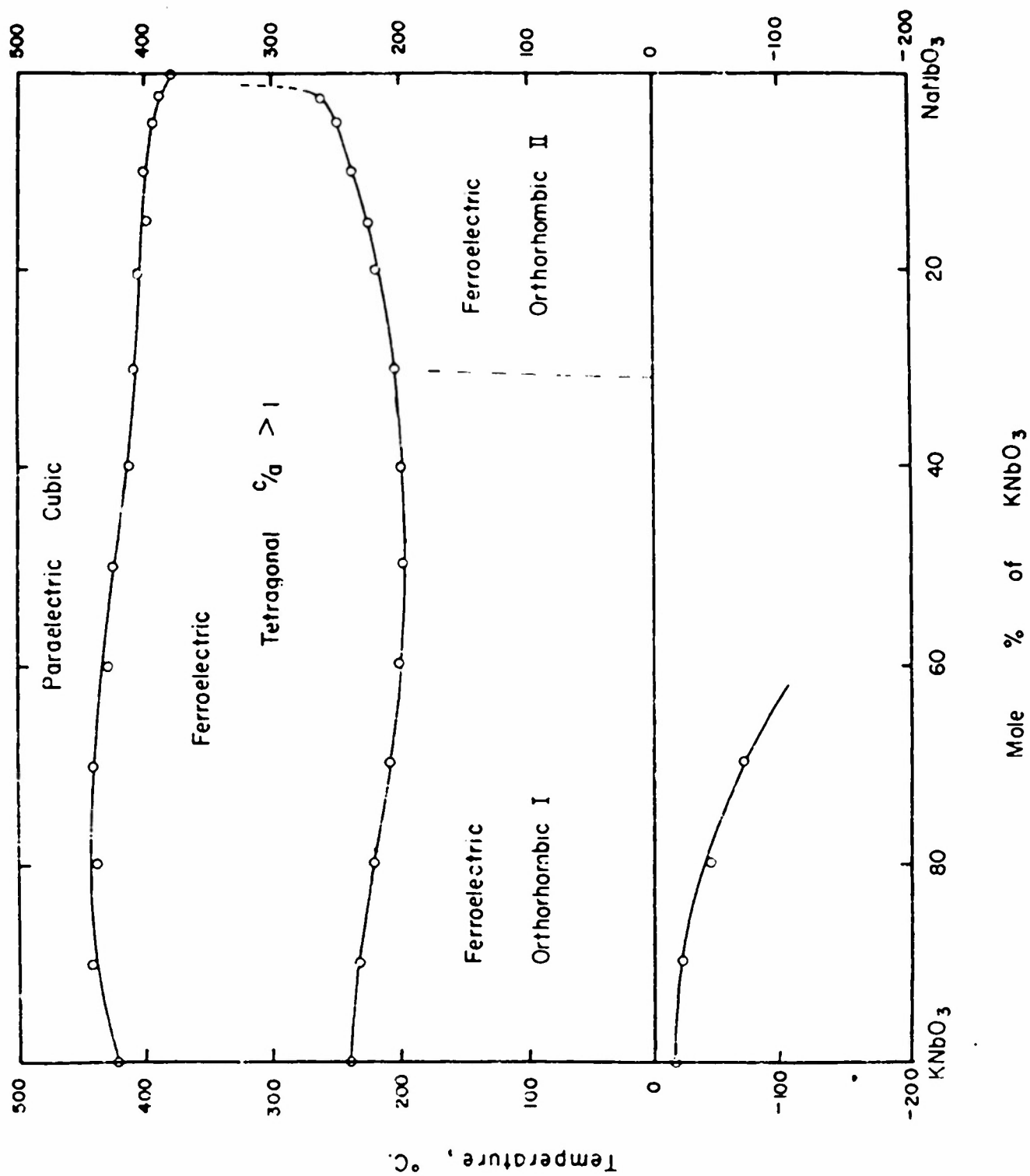


Fig. II

FIG. 12





250 °C.

KNbO₃

200 °C



390 °C.

(K₈₀-Na₂₀)NbO₃

190 °C.



320 °C.

(K₁₅-Na₈₅)NbO₃

190 °C.



270 °C.

(K₁₀-Na₉₀)NbO₃

200 °C.



350 °C

NaNbO₃

110 °C

Fig. 13

P-E RELATION OF (K-Na)NbO₃

In the lowest phase, we can get ferroelectric hysteresis loops, except for a region very close to pure NaNbO_3 ; but, comparing the loops of the same specimen at the intermediate phase, the coercive force is larger and the spontaneous polarization is smaller. As shown in Fig. 13, the hysteresis loop at the lowest phase becomes more and more ambiguous as we approach pure NaNbO_3 , although the solid solution such as $(\text{K}_{10}\text{-Na}_{90})\text{NbO}_3$ and $(\text{K}_{95}\text{-Na}_{05})\text{NbO}_3$ show good loops in the intermediate phase. No hysteresis loops were observed in pure NaNbO_3 . From these results we can conclude the paraelectric character of the highest phase, ferroelectricity in the middle phase, and also ferroelectricity in the lowest phase except for pure NaNbO_3 .

III. STRUCTURAL STUDY.

Before discussion of this phase diagram of the $(\text{Na-K})\text{NbO}_3$ system, we must examine the important point whether this $(\text{K-Na})\text{NbO}_3$ system is really forming a solid solution, because the difference of ionic radii of K and Na is large enough to give us this doubt.

(A) Crystal Structures at Room Temperature.

The crystal structures of KNbO_3 and NaNbO_3 at room temperature were studied by Wood⁽⁸⁾ and by Vonsden⁽¹¹⁾. Both crystals show the same type of orthorhombic distortion from cubic perovskite, but NaNbO_3 differs from KNbO_3 in one important point, namely, the patterns show "extra lines" which requires the assumption of some kind of superstructure. This superstructure was studied by Vonsden⁽¹⁰⁾, who reported the non-polar structure of this crystal, and drew some strange conclusions from this.

A series of powder photographs were taken with the various compositions covering the whole range of the $(\text{K-Na})\text{NbO}_3$ system. It is rather difficult

to get clearly resolved photographs especially on the NaNbO_3 side. This is presumably due to the large difference of ionic radii of K and Na, which inevitably causes a large internal strain. Especially on the NaNbO_3 side the replacement of the small Na ion with the large K ion may cause more strain than in the opposite case near KNbO_3 .

From the comparison of the photographs of whole solid solution range, we can reach following conclusions:

- (1) The lattice constant decreases gradually from KNbO_3 to NaNbO_3 , and no evidence was observed for the existence of a mixed phase.
- (2) Powder photographs of solid solutions ranging from KNbO_3 to $(\text{K}_{.50}\text{-Na}_{.50})\text{NbO}_3$ show sharp lines, and essentially the same characteristics as pure KNbO_3 .
- (3) From pure NaNbO_3 to $(\text{K}_{.15}\text{-Na}_{.85})\text{NbO}_3$, the diffraction patterns are essentially the same as pure NaNbO_3 , i.e., they show the same type of extra lines.
- (4) In the intermediate region between $(\text{K}_{.40}\text{-Na}_{.60})\text{NbO}_3$ to $(\text{K}_{.80}\text{-Na}_{.20})\text{NbO}_3$ the diffraction lines are rather diffuse, and it seems that the border-line between the two orthorhombic phases exists in this region. But the lattice constants show gradual changes even in this region.

(B) Lattice Change around the Transitions.

To examine the crystal structures of the intermediate phase and highest phase in the diagram shown in Fig. 12, we studied the temperature dependence of crystal structure of KNbO_3 , $(\text{K}_{.10}\text{-Na}_{.90})\text{NbO}_3$, and NaNbO_3 . The Unioam 19 cm. high temperature powder camera was used with Cu K α radiation.

The crystal structures of KNbO_3 at high temperatures were already studied by Wood, and our re-examination shows complete agreement with the previous data, giving the tetragonal structure with $c/a > 1$ between 220°C and

430°C, and the cubic structure above 430°C.

(K_{.10}-Na_{.90})NbO₃ shows the same lattice type at room temperature as NaNbO₃, and it changes to tetragonal lattice with $c/a > 1$ at the phase transition of 240°C, and extra lines seem to disappear at the same time. This tetragonal structure, therefore, is the same lattice type as in the intermediate phase of KNbO₃. The structure is cubic above 400°C.

The study of pure NaNbO₃ shows that this crystal is orthorhombic below 370°C, and the diffraction patterns taken above this temperature, e.g. 400°C, clearly show the lines of cubic perovskite. From this we can expect no more phase change at higher temperatures.

These results give the structural support for the phase diagram shown in Fig. 12.

IV. SPECIFIC HEAT MEASUREMENTS.

Specific heat vs temperature curves of KNbO₃, (K_{.10}-Na_{.90})NbO₃ and NaNbO₃ were measured by using an adiabatic calorimeter of Nagasaki-Takagi type⁽¹²⁾, which is an improvement of Sykes' calorimeter. Detail of the construction of this calorimeter was described in a preceding report⁽¹³⁾.

The specimen is a powdered ceramic prepared by the same method as the specimen for the dielectric and structural measurements. About 15 gms of material was placed in the Pt vessel, and heated at a rate of about 1°C/min. The heat content of the empty calorimeter was calibrated by using SiO₂ as a standard substance. The results are shown in Fig. 14 - 16.

From these curves we can easily see that NaNbO₃ and (K_{.10}-Na_{.90})NbO₃ show rather small anomalies compared with the relatively large anomalies in KNbO₃. By assuming a broken line shown in the figures as a normal specific

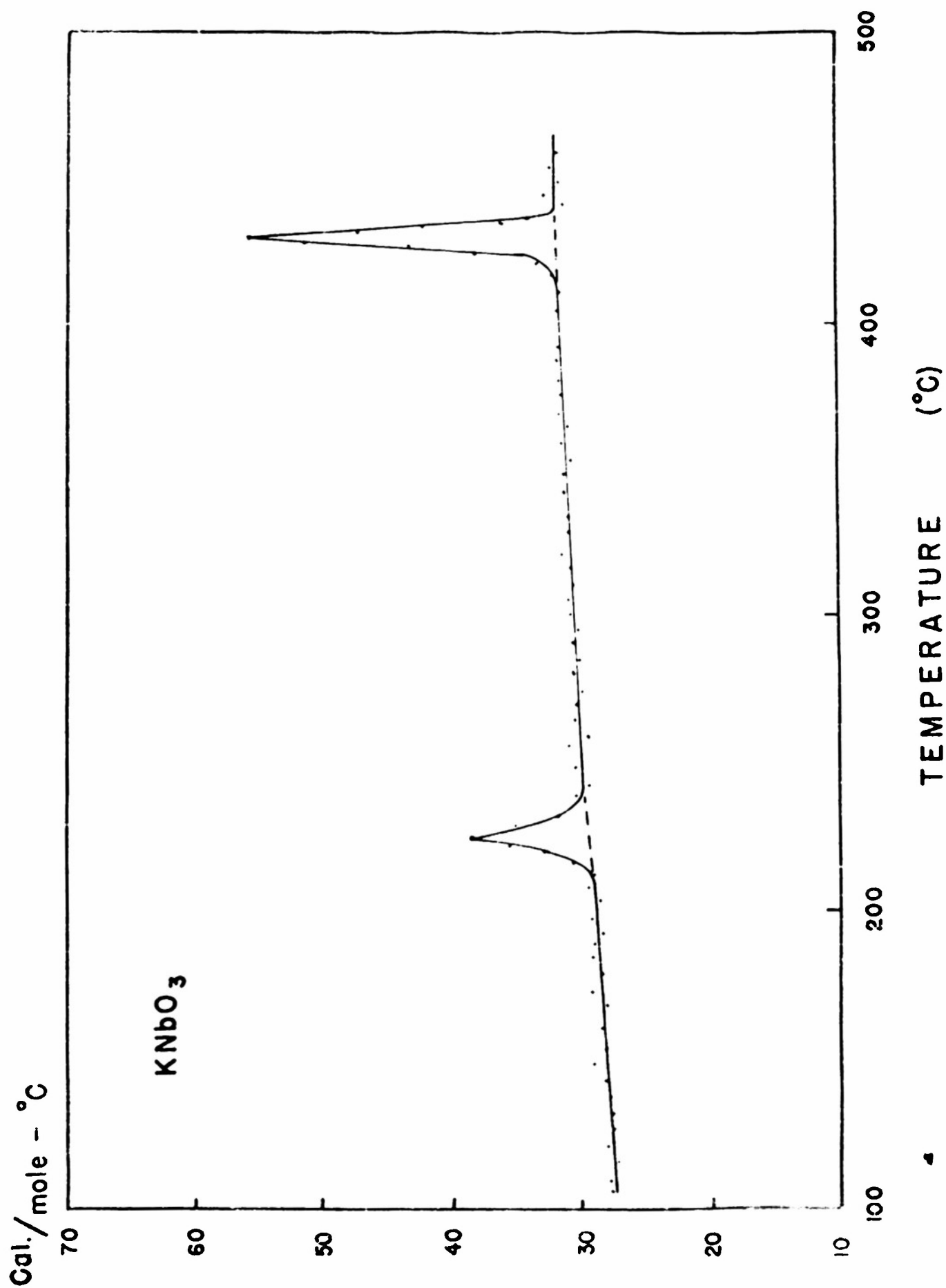


Fig. 14
SPECIFIC HEAT OF KNbO₃

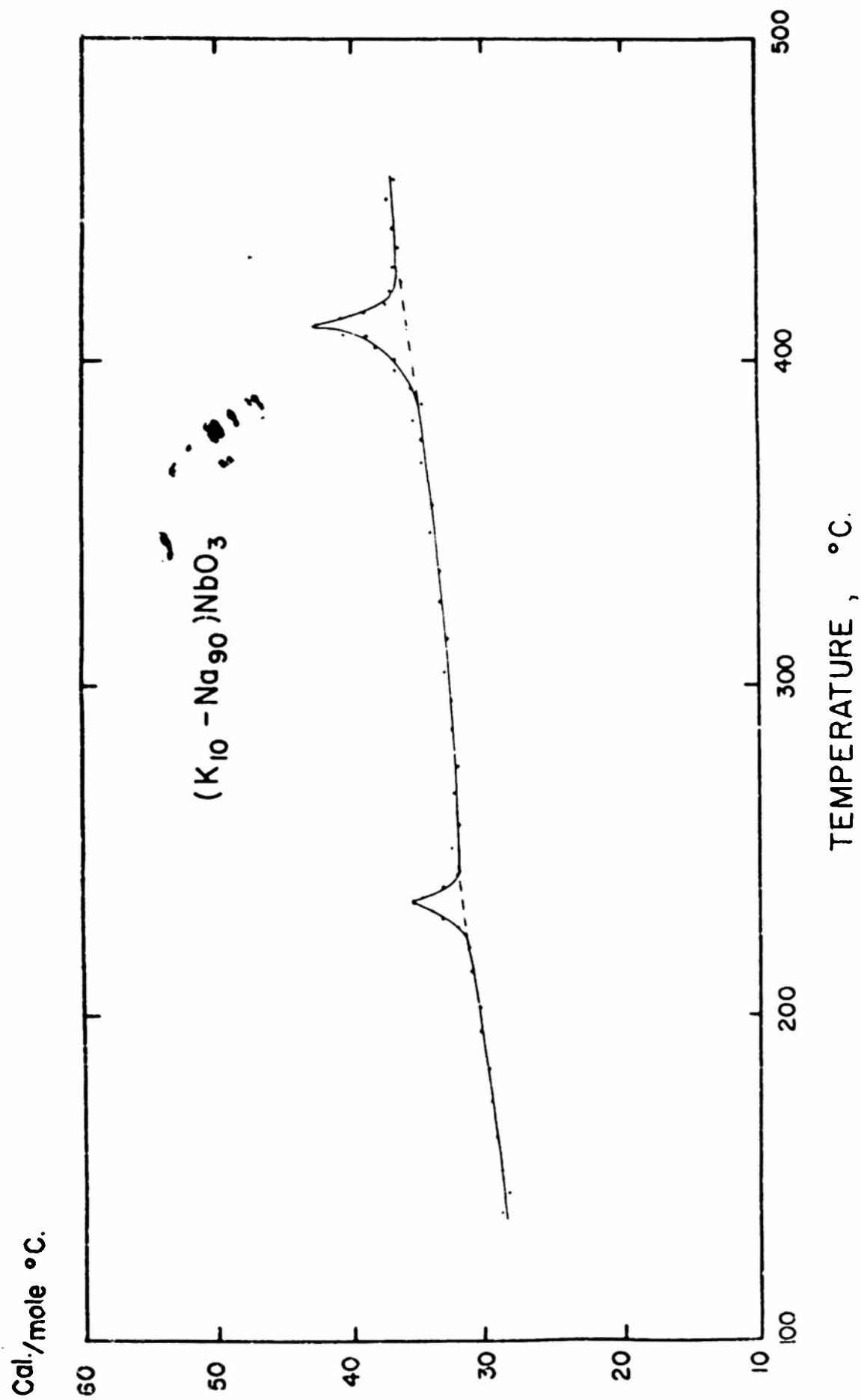


Fig. 15

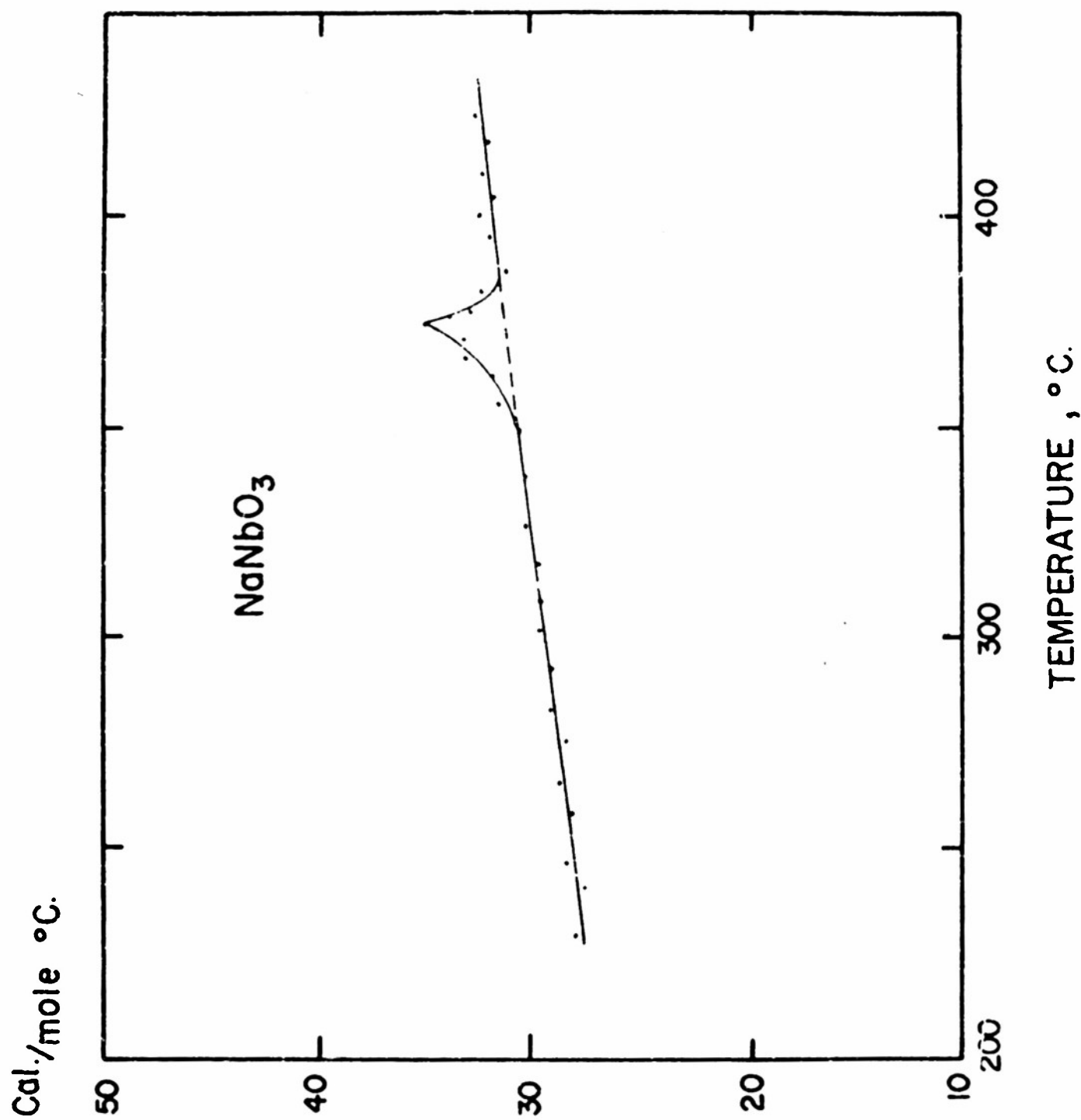


Fig. 16

heat curve, we can obtain the integrated transition energies as follows:

	lower phase change	upper phase change
KNbO_3	85 cal/mole	190 cal/mole
$(\text{K}_{.10}\text{-Na}_{.90})\text{NbO}_3$	20 cal/mole	60 cal/mole
NaNbO_3	-----	50 cal/mole

V. DISCUSSIONS.

Summarizing the above results, we can reach following conclusions:

- (1) NaNbO_3 shows only one phase transition at 370°C , accompanied by a structural change from orthorhombic to cubic.
- (2) When a small amount of Na is replaced by K, the ferroelectric intermediate phase can be observed. This phase shows a tetragonal lattice with $c/a > 1$, and it is the same phase as the intermediate phase of KNbO_3 .
- (3) Concerning the ferroelectricity of pure NaNbO_3 , though the phase diagram suggests ferroelectricity in this crystal, but the absence of detectable hysteresis loops gives us strong doubt. This problem is still open to question, and must await the further study.

We must add here the following results, obtained very recently, after completion of the study of $(\text{K-Na})\text{NbO}_3$ system using ceramic specimen. Single crystals of NaNbO_3 were prepared by the method used by Matthias and Remelka: namely, a mixture of NaNbO_3 , Nb_2O_5 and NaF was slowly cooled from 1500°C . Some of these single crystals show the dielectric anomalies at 370°C and 480°C in agreement with previous data and in contrast with our data on the ceramics. However, this phase change at 480°C may be explained by the small impurity contained in the crystal, because the phase diagram shown in Fig. 12 suggests that even small amount of impurity in NaNbO_3 can easily result in another phase

change. Up to now, no hysteresis loops were observed in NaNbO_3 single crystals. Further study of single crystals are now under way.

References

- (1) Cf. A. von Hippel, Rev. Mod. Phys. 22, 221 (1950).
- (2) G. H. Jonker and J. H. van Santen, Chem. Weekblad 43, 672 (1947);
G. Shirane and S. Hoshino, J. Phys. Soc. Japan 6, 265 (1951).
- (3) Sawaguchi, Shirane and Takagi, J. Phys. Soc. Japan 6, 333 (1951);
Shirane, Sawaguchi and Takagi, Phys. Rev. 84, 476 (1951).
- (4) H. D. Megaw, Proc. Phys. Soc. (Lond.) 58, 113 (1946).
- (5) Sawaguchi, Maniwa and Hoshino, Phys. Rev. 83, 1078 (1951).
- (6) G. Shirane, Phys. Rev. 86, 219 (1952);
G. Shirane and A. Takeda, J. Phys. Soc. Japan 7, 6 (1952).
- (7) B. Matthias and J. Remeika, Phys. Rev. 82, 727 (1951).
- (8) E. A. Wood, Acta Cryst. 4, 353 (1951).
- (9) R. Pepinsky, R. Thakur and C. McCarty, Phys. Rev. 86, 650 (1952).
- (10) P. Vousden, Acta Cryst. 4, 545 (1951).
- (11) P. Vousden, Acta Cryst. 4, 373 (1951).
- (12) S. Nagasaki and Y. Takagi, J. App. Phys. Japan 17, 104 (1948).
- (13) R. Pepinsky, Progress Report to Air Research and Development Command,
Contract No. AF33(038)-12645, Nov. 1, 1952.